HEDL-SA-1500FP
Conf-781022--38

MASTER

FUEL PINS AND CORE RESPONSE UNDER LMFBR TOP ACCIDENT CONDITIONS

by
N. P. Wilburn, D. E. Smith, R. E. Baars,
D. B. Atcheson*, and B. W. Spencer**

Hanford Engineering Development Laboratory
Richland, Washington 99352

* General Electric Company, Sunnyvale, CA
** Argonne National Laboratory, Argonne, IL

For presentation at the International Meeting on Nuclear Power Reactor Safety -- Topical Meeting, to be held in Brussels, Belgium, October 16-19, 1978

FUEL PINS AND CORE RESPONSE UNDER LMFBR TOP ACCIDENT CONDITIONS

N. P. Wilburn, D. E. Smith, D. B. Atcheson, R. E. Baars, and B. W. Spencer

BACKGROUND

Since the parametric analyses of the transient overpower (TOP) hypothetical core disruptive accident (HCDA) was done for the United States Fast Test Reactor (FTR),[1] new experimental information for TOP accident conditions has become available,[2] and many improvements in the TOP modeling have occurred including grouping techniques,[3] stochastic effects,[4] intrasubassembly incoherencies[5,6] and the Failure Potential (FP) correlation.[7]

With the implementation of the FP criterion into the MELT-IIIA[8] system, the predicted failure times occurred much later, 0.5 sec for a 0.5$/sec reactivity insertion. These results, confirmed using the BEHAVE code,[9] lead to a situation where more molten fuel and fission gas at failure exists in the pin. Much more molten fuel then flows into the channel, which results in a higher propensity for plugging if coherent failure is assumed, but will not necessarily result in a larger MFCI because much of the fuel will never contact the sodium since the flashing of some sodium upon initial contact with the molten fuel would drive the liquid sodium away from the rupture region, and the fuel will begin to pile up and form a molten mass with a very low surface area. From the standpoint of consistency, the formation of a plug necessitates a low subsequent MFCI with its attendant small movement of the lower interface and rapid reestablishment of flow. If a large MFCI were to occur, it is necessary that there be particle sizes of 200 to 400 microns in diameter, which would mean that the fuel was well fragmented and conditions for sweepout would pertain. It is therefore incompatible to assume that one has a large MFCI and no sweepout. Likewise, if one is to postulate a major blockage occurring, a small MFCI must follow.

If a coherent failure is assumed both in axial position and time, it will preferentially occur in the inner eight rows or to one side of the subassembly, as has been shown.[5,6] Due to the lower power-to-flow ratio in the outer row[5] or outer edge rows[6] these pins will most likely not fail, and if they do, they will fail much later and lower down. It was also noted[5] that the failures

that occur in the inner row of pins are all nominally directed toward the center, so the liquid fuel as it moves will move toward the center, leaving the outer circumferential area and lower power side of the subassembly relatively free.

EXPERIMENTAL RESULTS

Out-of-reactor experiments which show this scenario are currently being performed at Argonne National Laboratory to examine fuel sweepout and related post-failure phenomena under hypothetical TOP accident conditions. These tests are supplementing the TREAT MARK-II loop data base by keying on effects of important parameter variations such as system hydraulics and intrabundle coherency. In these tests, molten UO_2, generated by a thermite reaction at 3470°K, is injected over approximately 40 msec into flowing sodium in a bundle of simulated LMFBR-type fuel pins. Hydraulic conditions in the bundle are selected to match conditions in either the MARK-II loop (HUMP-series) or the current design LMFBR subassembly (CAMEL-series). To date, four tests have been performed in both single-pin and seven-pin configurations representing coherent and incoherent subassembly power-to-flow cases, respectively. Test conditions are listed in Table 1. Details of the fuel motion were observed using a flash X-ray cine system.

Table 2 presents a compilation of significant findings from the four sweepout tests. In each test the channel pressurized upon the onset of injection to higher than the driving (inlet plenum) pressure. This typically results in decelerations of the sodium entering the pin bundle, as evident from flow rate data in Figure 1, but does not cause immediate reversal due to the momentum of the incoming flow. If the inlet flow momentum is small, the flow is readily reversed and the intermixing needed for sweepout may not be established. This occurred only in the HUMP one-pin test, where the inlet inertia length was only 0.59 m; no fuel sweepout occurred in this test. Hence, a necessary condition for sweepout is that sodium flow continues through the bundle, by its inertia, in the presence of short duration (5-10 msec) adverse pressure gradients which occur upon pin failures. This requirement was satisfied for the other tests in the series and is expected to be satisfied in the subassembly.

TABLE 1. Conditions for ANL CAMEL and HUMP-series Fuel Sweepout Tests; T_i = 500°C.

COHERENCY \ SYSTEM MOCKUP	TREAT MARK-II LOOP	LMFBR SUBASSEMBLY
One-dimensional (Coherent)	HUMP ONE-PIN U_o = 3.5 m/sec ΔP = 0.062 MPa L* = 0.59 m m_f = 12.9 g	CAMEL C2 (ONE-PIN) U_o = 7.6 m/sec ΔP = 0.79 MPa L* = 1.93 m m_f = 9.4 g
Two-Dimensional (Incoherent)	HUMP SEVEN-PIN U_o = 3.5 m/sec ΔP = 0.08 MPa L* = 1.41 m m_f = 23.7 g	CAMEL C3 (SEVEN-PIN) U_o = 6.7 m/sec ΔP = 0.81 MPa L* = 2.81 m m_f = 27.3 g

TABLE 2. Summary of Results from ANL CAMEL and HUMP-series Fuel Sweepout Tests

	HUMP 1-Pin	HUMP 7-Pin	CAMEL 1-Pin	CAMEL 7-Pin
Mass of fuel injected, g	12.9	23.7	9.4	27.3
Initial channel pressurization, MPa	0.5	1.4	1.4	1.7
Flow reversal	yes	yes	no	no
Number FCI's	none	2	2	4
Fuel sweepout, g	none	6.2	3.5(est.)	8.55
Mass of fuel in blockage, g	12.9	17.3	4.8	18.6
Flow recovery	17%	80%	70%	94%
Calculated area blockage	-	68%	84%	60%

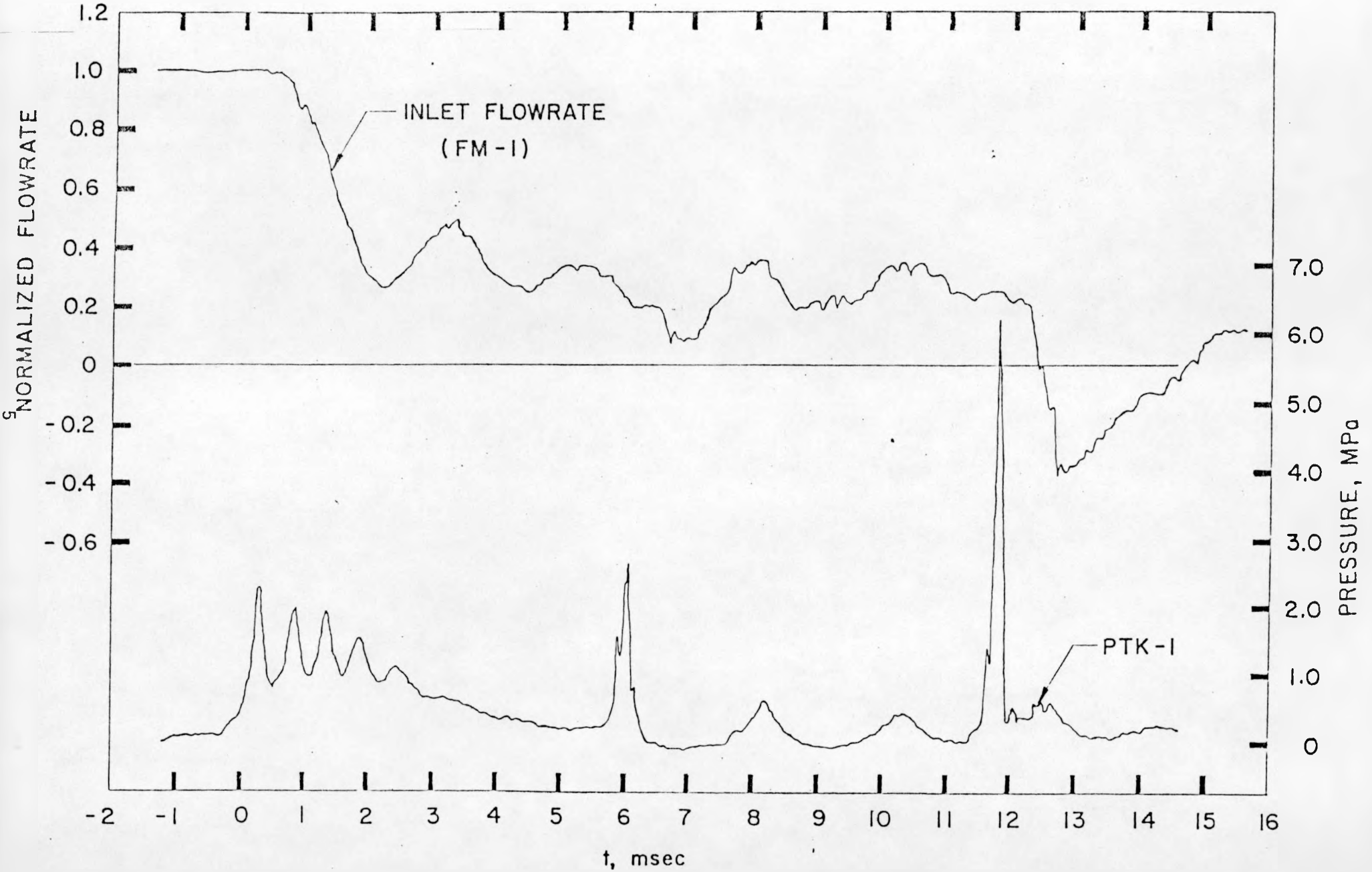

FIGURE 1. Inlet Flowrate and Interaction-zone Pressure on Expanded Time Scale: HDMP-7

In the other three tests, coolant flow continued through the bundle as molten fuel was injected. This resulted in a forced impingement of the flowing sodium into the underside of the region where molten UO_2 was accumulating. The flash X-ray pictures of fuel motion in these cases appear to show a stagnation type flow for the fuel as it first impacts on adjacent pins; that is, it appears to spread uniformly upward and downward in the channels at this early stage of the injection. This behavior is consistent with analysis[10] which has shown that breakup of the liquid fuel and momentum exchange with the sodium would not result in significant downstream deflection before the fuel impacts on nearby cladding surfaces. Hence, the behavior of the injected fuel becomes dependent upon other forces present, notably (a) the buildup of ΔP across the fuel region as the fuel accumulation tends toward complete plugging, and (b) the incidence of FCI's.

The ΔP buildup is determined by the coherency of pin failures across the subassembly. When such failures occur coherently across the region, the local axial pressure gradient is sharply increased, resulting in acceleration of the accumulated fuel in the downstream direction. This type of behavior was observed for the initial fuel motion in the CAMEL C2 test (subassembly hydraulics, 1-D case), and can be discerned in the flash X-ray pictures. Immediately after the onset of injection, the fuel spanned the coolant annulus horizontally, impacting on the pin without showing preferential deflection upward or downward. By 4 msec later, the fuel had wrapped around the pin perimeter and was deflecting downstream. Test data showed the pressure drop across the fuel region had built up to about 0.16 MPa, producing the onset of sweepout.

In contrast, when pin failures occur incoherently across the region, a bypass flow regime develops which precludes the local ΔP buildup. Due to the variation of power-to-flow across the LMFBR subassembly, the subassembly is expected to behave in this manner. This case was examined in the two seven-pin tests, in which the fuel was injected laterally into three rows of pins, representing the outer overcooled rows of pins in the subassembly whose failures are expected to lag behind the inner row failures. This type of fuel motion was observed in the seven-pin HUMP X-ray pictures. The injected fuel traveled laterally between the

first and second row of pins and spread upward and downward uniformly in the central channels. The sequence of frames when flashed in rapid succession, clearly shows an upward ejection of dispersed fuel through the central channels of the bundle. The mechanism for fuel sweepout may have involved the impulses imparted by the two FCI's which occurred at 5.7 and 11.5 msec in this sequence, as monitored by the test section pressure transducers (quartz piezoelectric).

Small-scale fuel-coolant interactions occurred in each of the three tests where sodium flow continued beyond the first few milliseconds of the injection. Between two and four such occurrences were recorded in each of these tests from as early as 2.7 msec to as late as 80.5 msec after the onset of injection. The pressures of these events ranged up to 18 MPa peak and were less than 1 msec duration. In nearly every instance, the effect of the pressurization event was to abruptly reduce, and in some cases momentarily reverse, the inlet sodium flow. In all cases the flow rate quickly recovered, and the events themselves caused negligible upstream voiding or vapor blanketing effects. In each of the three tests, upward fuel dispersal was observed to be triggered by some of the FCI's. This is most clearly seen in the single-pin C2 test, where an FCI at 10.0 msec caused upward ejection of nearly all the fuel in the channel at that time. In this test, the FCI-driven dispersal acted in addition to the hydraulic sweepout which was already underway. In the two seven-pin tests, the FCI-driven dispersal appeared to be the only mechanism to give sweepout. In all three cases, the sweepout was impressive, amounting to greater than 25% of the injected fuel.

Recent analysis of fuel/cladding energy transfer in the hypothetical TOP accident[11] has indicated that cladding failures in the subassembly would not be independent of one another; fuel ejected from one pin onto neighboring pins would hasten the failures of those pins. The variation in failure times would be reduced from the order of 0.1 sec (stochastic variation)[4] to the order of 0.01 sec. Hence the overall coherent versus incoherent behavior of the system depends in part on the lateral spread of molten fuel from the central region of the subassembly to the outermost overcooled rows. In the HUMP seven-pin test, the fuel did not effectively penetrate past the second row of pins. However, the outermost row was contacted and some melting attack was observed. In the CAMEL seven-pin test, the lateral fuel penetration was more complete; fuel accumulated all

the way to the far wall of the test section. Although this aspect of test data is neither complete nor definitive, there is indication that the lateral spread of fuel to the outer pin rows may also act to lessen the overall failure incoherencies.

In general, nearly all the fuel which underwent sweepout was swept completely above the tops of the simulated fuel pins. Very little was deposited along the upper pin structure as it was swept upward. The remaining fuel accumulated locally in the coolant channels, freezing on the cladding and structure to form partial channel blockages. These blockages were substantial in terms of effective area plugged ($\geq$ 60% in all tests). However, their incremental pressure drop was generally small relative to the system overall pressure drop so that the effect on sodium flow rate was considerably less. This was particularly true of the two seven-pin tests in which flow rate recovery was 80% and 94% complete. Even in the single-pin C2 test in which the blockage encompassed effectively 84% of the channel, the flow recovery was 70% complete. In all the tests the partial blockage could be characterized as two distinct regions: (a) an effectively unobstructed passage(s) through which nearly all the coolant flow was channeled, and (b) a region of accumulated fuel which in a few instances was very dense but more generally was itself quite porous. Larger bundle tests are required to better characterize the blockage formations.

In summary, these out-of-reactor CAMEL- and HUMP-series sweepout tests have revealed the following:

(1) The hydraulics of the system are important to sweepout since positive coolant flow must be maintained long enough for sweepout-related forces to develop. This requirement appears to be satisfied in the current-design LMFBR subassembly.

(2) A significant amount of fuel removal occurred in each of the three tests in which sustained sodium flow, characteristic of subassembly behavior, was attained.

(3) When the bundle behaves nominally one-dimensionally (coherent case), the buildup of an axial pressure gradient across the molten fuel, which in the extreme may equal the pump head, provides a mechanism for hydraulic sweepout.

(4) Small-scale, local FCI's are consistently produced when sodium flow is sustained into a region of accumulating molten fuel.

(5) FCI's have been observed to trigger fuel sweepout independent of the presence or absence of hydraulic-related sweepout force; this provides a sweepout mechanism in the two-dimensional, incoherent case.

(6) No large-scale, energetic FCI's have been produced. The small-scale FCI's have caused only momentary, and generally negligible, upstream voiding or vapor blanketing.

(7) Swept-out fuel was generally carried beyond the tops of the pins, and plate-out along the pin structure was not observed.

(8) Partial channel blockages were typically formed at the interaction zone from fuel which had not been swept away.

(9) The blockages contained macroscopic porosity through which the sodium flow was channeled; the flow rate recovery was greater than 70% complete for conditions applicable to the subassembly.

ANALYTICAL RESULTS

From the above experimental results where no large scale FCI's and little or no flow reversal was observed, it is to be expected that the outer rows of pins in an LMFBR subassembly will have continual liquid cooling and will not fail, as has been demonstrated before.[5,6] However, if a larger FCI occurs (which is logically inconsistent as stated earlier) the outer pins will be vapor-blanketed and will ultimately fail, but several centimeters closer to the axial midplane. It is possible, therefore, that another plug will occur on the outer pins, but it will be in a different axial location. Thus, in both the case where the outer pins do not fail and in the case where they do fail, flow should be reestablished because the channel is still open. In the first case, there is no blockage in the outer area of the subassembly, and in the seond case the outer blockage is axially displaced from the inner blockage by several centimeters.

When the flow is reestablished, some coolant vaporization could occur when the sodium hits the fuel debris caused by failure of the outer pins. However, the full pressure of the pumps is still available, and this should allow the eventual reestablishment of flow.

In order to analytically investigate the details of this scenario in the FTR for the assumed case of coherent failure in axial position and time, first for the inner pins and then for the outer pins, a computer run was designed using a special version of MELT-IIIA with the new grouping technique and the FP criterion where an MFCI was permitted which resulted in vapor blanketing of the outer pins and their failure. The inner eight rows of pins in the subassemblies were lumped together and treated as a single channel. The outer ninth row of pins was treated as an adjacent channel of index one number higher. The flow rates for the inner and outer channels were balanced so that the temperature increases were correct. No mixing was assumed to occur between the inner and outer channels up to the time of pin failure.

At the time when the inner channel failed, the FCI zone was assumed to blanket both the inner channel and outer channel pins, and the upper and lower interface as calculated for the inner channel was assumed to be carried over to the outer

channel. The calculation of the hydraulics for the outer channel was discontinued, and the conditions in the inner channel were simply mapped onto the outer channel.

After failure occurred in the inner channels, the Failure Potential value was tracked for the outer channels to determine when, where, and if failure would occur for the outer channels. However, the control variables in the MELT code indicating failure for the outer channels were suppressed in order to track the run as far as possible with the system. The logic behind this decision was that if failure did occur in the outer channels, the fuel motion would be into a voided channel and there would be little or no contribution to the MFCI. Furthermore, the failure location would be such that there would be either some additional negative reactivity contribution or very little effect at all.

The results for reactivity behavior as a function of time are presented in Figure 2 for a 0.5$/sec reactivity insertion. The final reactivity value shown of -7.5$ for the fuel motion is due exclusively to the fuel motion from the center of the pin to the failure points. Ultimately when the reactor returns to steady-state power conditions and the Doppler is back to zero, with a total insertion of 4.0$, addition of the contributing reactivities of -7.5$ for the fuel plus 0.6$ for the Doppler return feedback leads to the conclusion that the reactor will be a total of 2.9$ shutdown. Ultimately, once the precursors have decayed away, the reactor will end up with only decay heat power (at a subcritical state somewhat less than the stated value due to some positive Doppler and structural feedback upon cooldown). The power trace is shown in Figure 3. It peaks out at approximately 2550 MW, just before the first channel fails. It decays away to approximately 100 MW during the course of the transient shown. This lingering power is due essentially to the flux level dictated by the slowly decaying precursors.

Figure 4 is presented to show the behavior as a function of axial position for the Failure Potential calculation. The dashed curve is the axial variation of the Failure Potential in Channel 1 at the time of initial failure, which is at 2.9805 sec. The Failure Potential axial variation for outer Channel 2 is shown at several successive times, and shows a bowing out toward the axial center such that failure is predicted to occur in node 13 (each node = 5.08 cm). Inspection of these

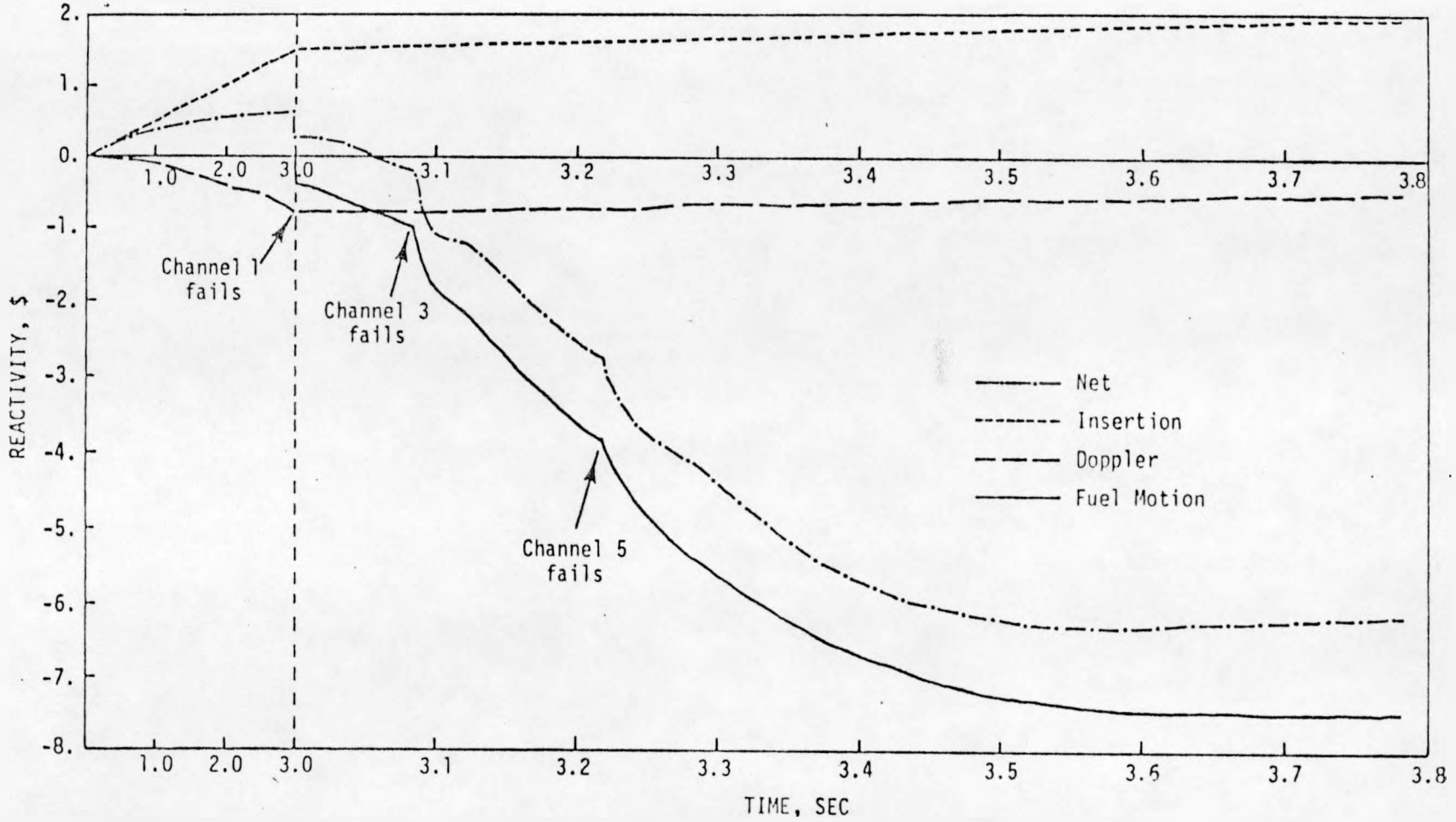

FIGURE 2. Reactivity vs. Time for a Large MFCI in Split-Channel Runs. (Neg. No. 7710588-12)

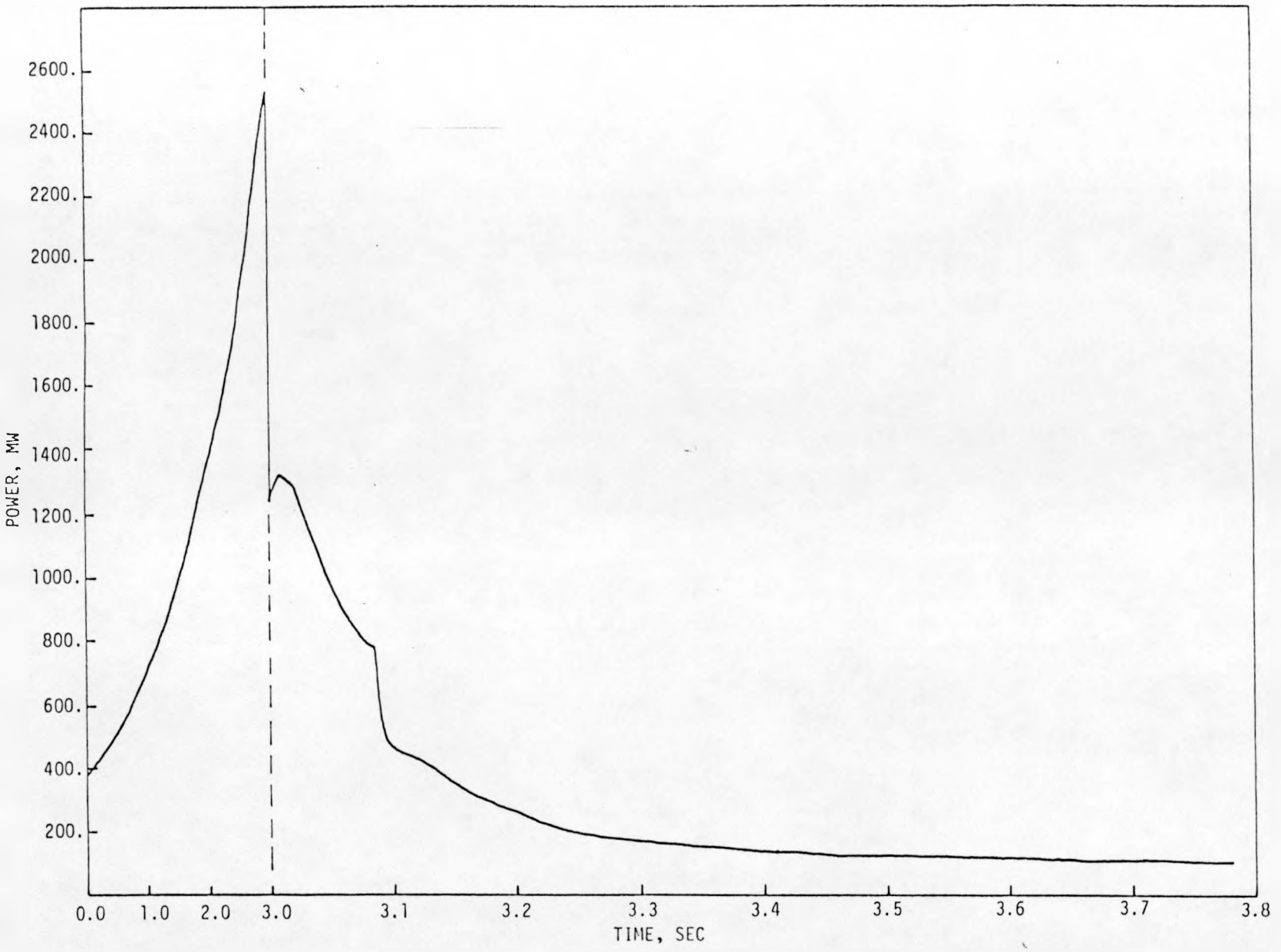

FIGURE 3. Power vs. Time (0.5$/sec TOP) for a Large MFCI in Split-Channel Runs. (Neg. No. 7710588-6)

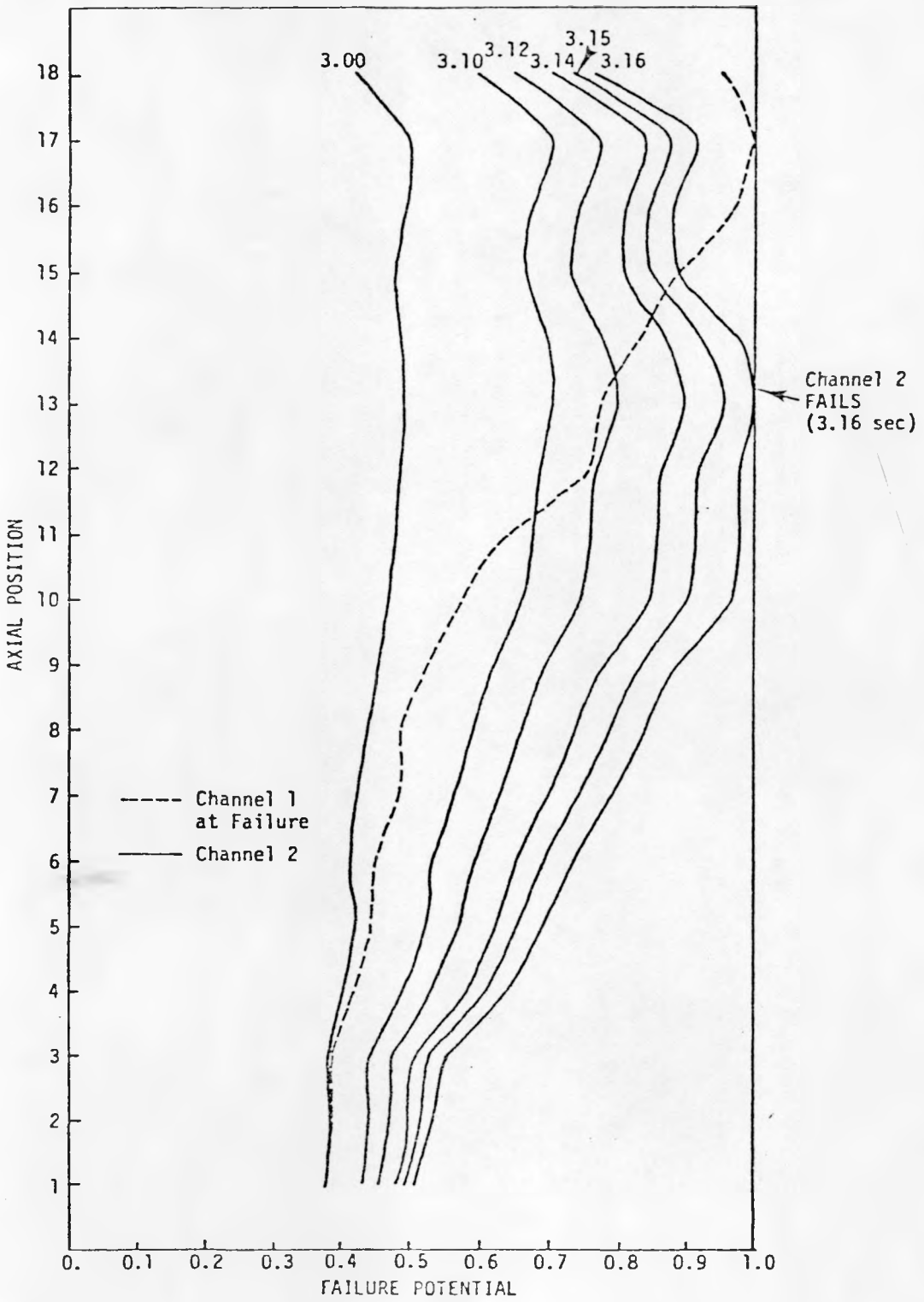

FIGURE 4. Axial Variation Failure Potential for Channels 1 and 2 (0.5$/sec TOP) for a Large MFCI in Split-Channel Runs. (Neg. No. 7710588-25)

curves show that there is little chance that the failure would occur in a node higher than node 13; however, the failure location might move as low as node 12. Thus, for this case the difference in failure locations between the inner and outer channels is four nodes (which corresponds to 20 cm in the reactor). Thus, if the outer channel fails as calculated here, the fuel will be discharged at a point 20 cm lower on the outer pins than it would on the inner pins, thus leaving a channel open to coolant by a winding process through the two postulated blockages.

Figure 5 is presented to show the interface position as calculated for Channels 1 and 2. The interface during the course of the calculation is assumed to be the same in both the inner and outer channels. The channel is completely refilled with coolant after about 400 msec. The effects of the assumed large MFCI are apparent in the large voiding beyond the plenum area into the pool above the subassembly. The break noted in the upper interface curve is due to the vapor bubbles passing into the upper liquid pool.

The break noticed in the lower interface curve is a result of boiling occurring off the lower interface due to the low pressures existing in the MFCI zone. The pressures are of the order of 0.5 to 1.0 atm, corresponding to a sodium vapor temperature of about 1100°K, and the liquid temperatures at this point run at approximately 1300°K, which causes vaporization off the lower interface. It should be noted that the calculated coolant reentry curves are fairly smooth, since the current modeling capability does not allow for pressure fluctuations that might arise from localized fuel/coolant interactions surrounding the regions of postulated blockage.

CONCLUSION

The conclusion of this updated scenario for the TOP HCDA is still generally the same as the earlier assessment[1] for the FTR and hence for LMFBR's in general. Only a few subassemblies would be affected, and the overall consequences would be benign. The transient would be terminated by fuel relocation away from the core midplane and long-term coolability should be maintainable.

move to Page 1 as second paragraph. CPC 8/21/78

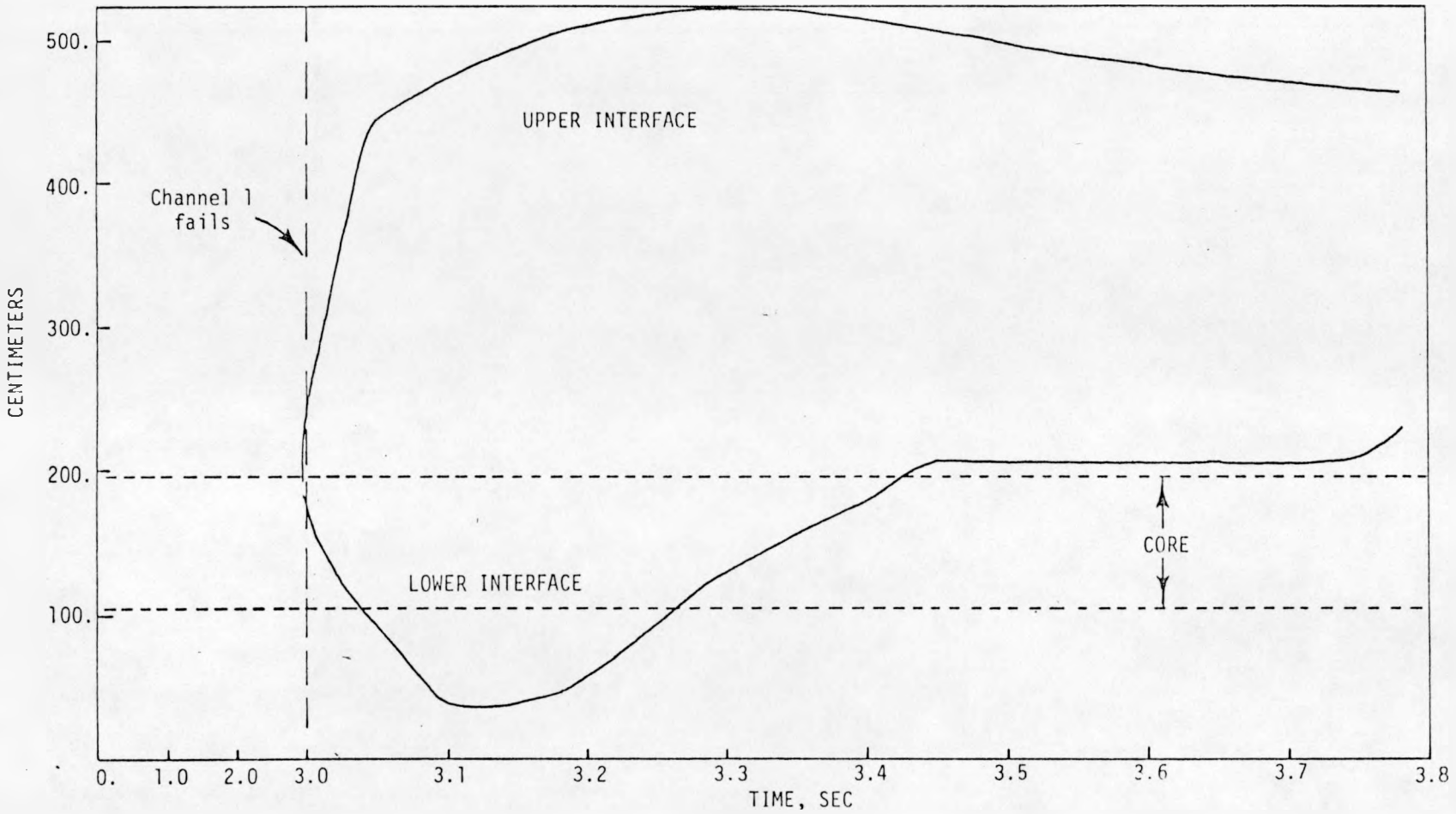

FIGURE 5. Interface Position - Channels 1 and 2 (0.5$/sec TOP) for a Large MFCI in Split-Channel Runs. (Neg. No. 7710588-9)

REFERENCES

1. A. E. Waltar and N. P. Wilburn, et al., An Analysis of the Unprotected Transient Overpower Accident in the FTR, HEDL-TME 75-50, Hanford Engineering Development Laboratory, Richland, WA, June 1975.

2. B. W. Spencer, L. Bova, G. T. Goldfuss, D. Raridon, R. E. Henry, and D. R. Armstrong, "CAMEL Single-Pin Fuel Sweepout Test C2," Trans. ANS, 27, p. 503, (1977).

3. N. P. Wilburn, Improved Subassembly Grouping for Multi-Channel TOP HCDA Safety Analysis, HEDL-TME 77-25, Hanford Engineering Development Laboratory, Richland, WA, July 1977.

4. N. P. Wilburn, et al., "Sensitivity of LMFBR Hypothetical Accident Analysis Variations in an Empirical Fuel Pin Failure Criterion," Proc. CONF-761001, Vol. 3, pp. 988-997, (1976).

5. S. C. Yung and N. P. Wilburn, "Failure Pattern Within an FTR Subassembly Under a TOP Accident," Trans. ANS, 27, p. 536, (1977).

6. S. C. Yung and N. P. Wilburn, "Effect of Power Skew on the FTR TOP Accident," Trans. ANS, 28, p. 475, (1978).

7. R. E. Baars, "HEDL Empirical Correlation of Fuel Pin TOP Failure Thresholds -- Status 1976," Proc. CONF-761001, Vol. 4, pp. 1673-1678, (1976).

8. C. H. Lewis and N. P. Wilburn, MELT-IIIA: An Improved Neutronics, Thermal-Hydraulics Modeling Code for Fast Reactor Safety Analysis, HEDL-TME 76-73, Hanford Engineering Development Laboratory, Richland, WA, December 1976.

9. R. R. Sherry and D. B. Atcheson, User Manual for the BEHAVE-SST Fuel Rod Mechanics Program, GEFR-00001, General Electric Company, Sunnyvale, CA, February 1977.

10. B. G. Jones, B. W. Spencer, and R. E. Henry, "Fragmentation Dynamics of Molten UO_2 in Sodium Under TOP Accident Conditions," Trans. ANS, 27, p. 497, (1977).

11. B. G. Jones, B. W. Spencer, and R. E. Henry, "Interaction of Molten UO_2 with Stainless Steel Cladding Under TOP Accident Conditions," TANSAO 28, p. 477, (1978).